CHIN.PHYS.LETT. Vol. 17, No. 10 (2000) 775

Computational Analysis of the Vertical Bridgman Growth of Te Doped GaSb Under Microgravity *

LIU Yong-Cai(刘永才)[1,2], CHEN Wan-Chun(陈万春)[1,3], GE Pei-Wen(葛培文)[1], HUO Chong-Ru(霍崇儒)[1]
[1]Institute of Physics, Chinese Academy of Sciences, Beijing 100080
[2]School of Chemical Engineering, Tianjin University, Tianjin 300072
[3]National Microgravity Laboratory, Chinese Academy of Sciences, Beijing 100080

(Received 3 December 1999)

A transient analysis of Te doped GaSb melt growth process is performed using finite element method. The solute concentration at the growth interface increases with time because of $k < 1$. The growth interface shape becomes a little flat at the beginning of the growth compared with the initial shape. Radial segregation occurs even under the μg condition. This segregation increases with the increase of gravity when gravity is small, and reaches a maximum at $g = 10^{-3}$ for our system.

PACS: 81.10.Mx, 61.72.Ss, 02.70.Dh

GaSb-based semiconductors are very good substrate materials for electronic and optoelectronic devices. Considerable efforts have been made to grow high quality GaSb single crystals. One of these efforts is the employment of microgravity environments[1,2] because of the relatively low melting point of GaSb among the semiconductors. In this study, we present a numerical analysis of Bridgman growth of Te doped GaSb crystals under microgravity in order to better conduct the future space experiments.

Table 1. Physical properties and operating conditions (subscripts s, m, and a represent solid, melt, and ampoule, respectively).

Description	Symbols and values
Density	$\rho_s = 5.7 \times 10^3\,\mathrm{kg/m^3}$
	$\rho_m = 6.0 \times 10^3\,\mathrm{kg/m^3}$
	$\rho_a = 2.2 \times 10^3\,\mathrm{kg/m^3}$
Diffusion coefficient	$D_m = 4 \times 10^{-9}\,\mathrm{m^2/s}$
Thermal conductivity	$k_s = 7.81\,\mathrm{W/m{\cdot}K}$
	$k_m = 17.1\,\mathrm{W/m{\cdot}K}$
	$k_a = 3.5\,\mathrm{W/m{\cdot}K}$
Thermal expansion coefficient	$\beta = 9.6\times10^{-5}\mathrm{K}^{-1}$
Kinematic viscosity	$v = 1.4 \times 10^{-7}\,\mathrm{m^2/s}$
Specific heat	$C_{p,m} = 328.0\,\mathrm{J/(kg{\cdot}K)}$
Heat of fusion	$\Delta H_f = 1.36 \times 10^6\,\mathrm{J/kg}$
Melting temperature	$T_{mp} = 985.0\,\mathrm{K}$
Equilibrium segregation coefficient	$k = 0.30$*
Heat transfer coefficient	$h = 3.2\,\mathrm{W/m^2{\cdot}\,K}$
Emissivity	$\varepsilon_{ag} = 0.5$
Furnace temperature gradient	$G = 30\,\mathrm{K/cm}$
Ampoule outer length	$L = 21\,\mathrm{cm}$
Ampoule inner radius	$R = 1.5\,\mathrm{cm}$
Ampoule thickness	$d = 0.5\,\mathrm{cm}$
Length of insulation zone	$L_I = 5.0\,\mathrm{cm}$
Furnace translation rate	$V_p = 7.56\times\ 10^{-7}\,\mathrm{m/s}$

*Te in GaSb (Ref. 13).

We consider a generic vertical Bridgman growth system. As depicted in Fig. 1, a cylindrical ampoule filled with Te doped GaSb melt is contained in a vertical gradient furnace, and solidification proceeds from the bottom of the ampoule as the ampoule is translated downward. The physical properties and operating parameters of this system are listed in Table 1

The governing equations are cast in dimensionless form using the following scalings: temperature $T \equiv \widetilde{T}/T_{mp}$, melt velocity $\boldsymbol{v} \equiv R\widetilde{\boldsymbol{v}}/\alpha_m$, time $t \equiv \widetilde{t}v/R^2$, pressure $p \equiv R^2\widetilde{P}/(\mu\alpha_m)$, solute concentration $c = \widetilde{c}/c_0$, and gradient operator $\nabla \equiv R\widetilde{\nabla}$, with T_{mp} denoting the melting point, $v(=\mu/\rho)$ the kinematic viscosity of the melt, R the radius of the ampoule, μ the viscosity of the melt, c_0 the initial concentration, $\alpha_m(=k_m/(\rho C_p)_m)$ the thermal diffusivity of the melt, ρ the density, and C_p the specific heat. Time-dependent heat transfer in crystal and ampoule can be given in dimensionless form as

$$Pr\Gamma_i\frac{\partial T}{\partial t} - \nabla^2 T = 0, i = s, a \tag{1}$$

where Pr is the Prandtl number (v/α_m), Γ_i is the ratio of thermal diffusivities of the melt to solid and ampoule when $i = s$, a, respectively.

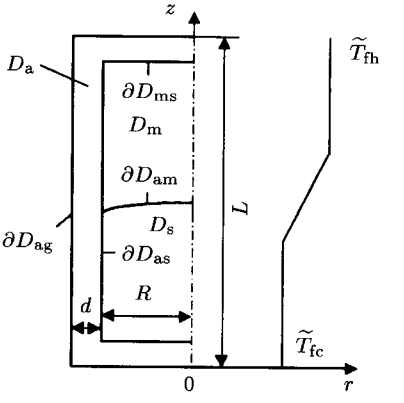


Fig. 1. Schematic of the vertical Bridgman growth system.

The dimensionless equations governing momentum, heat and solute transfers in the melt are

$$\frac{\partial \boldsymbol{v}}{\partial t} + \frac{1}{Pr}\boldsymbol{v}\cdot\nabla\boldsymbol{v} + \nabla P - \nabla^2\boldsymbol{v} - Ra(T-1)\boldsymbol{e}_r = 0 \tag{2}$$

$$\nabla\cdot\boldsymbol{v} = 0 \tag{3}$$

$$Pr\frac{\partial T}{\partial t} + \boldsymbol{v}\cdot\nabla T - \nabla^2 T = 0, \tag{4}$$

$$\frac{\partial c}{\partial t} + \frac{1}{Pr}\boldsymbol{v}\cdot\nabla c - \frac{1}{Sc}\nabla^2 c = 0 \tag{5}$$

*Supported by the Climbing Project of the National Ministry of Science and Technology (95-Yu-34), and the Foundation of National Ministry of Education.
©by the Chinese Physical Society

where $\boldsymbol{e}_r$ is the unit vector in the r-direction, Ra and Sc are the Rayleigh number $[g_0 g\beta T_{mp} R^3/(\alpha_m v)]$ and Schmidt number (v/D_m), respectively, with g_0 the gravity on the earth, g the gravity factor, and β the thermal expansion coefficient of the melt.

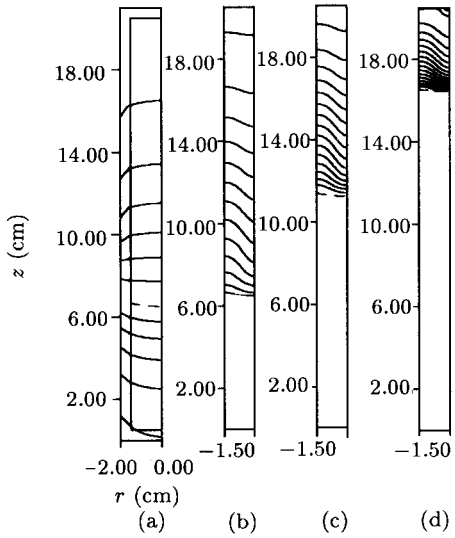


Fig. 2. Temperature and concentration distribution under $g=10^{-5}$. The dashed lines represent the melt/crystal interface. (a) Temperature distribution at $\tilde{t}=6.25\times10^4$ s, with $\Delta\tilde{T}=10$ K; (b) Concentration distribution at $\tilde{t}=6.25\times10^4$ s, with $c_{max}=1.58$, $c_{min}=1.0$, $\Delta c=0.045$; (c) Concentration distribution at $\tilde{t}=1.25\times10^5$ s, with $c_{max}=2.33$, $c_{min}=1.07$, $\Delta c=0.085$; (d)Concentration distribution at $\tilde{t}=1.875\times10^5$ s, with $c_{max}=3.16$, $c_{min}=1.18$, $\Delta c=0.13$.

Boundary conditions on the melt/crystal interface include the energy balance: $(-K_m\nabla T_m + \nabla T_s)\cdot\boldsymbol{n}_{ms} = Pe_s$; the solute balance: $(\nabla c_m)\boldsymbol{n}_{ms} = Pe_c c_m(k-1)$; as well as the equilibrium condition: $T=1$; where K_m is the dimensionless thermal conductivity $(K_m=k_m/k_s)$, $\boldsymbol{n}$ is the unit normal vector, k is the equilibrium segregation coefficient, c_m is the concentration of solute in the melt at the interface. Pe_s and Pe_c are respectively given as $Pe_s=RV_n\Delta H_f\rho_s/(k_sT_{mp})$ and $Pe_c=RV_n/D_m$, with ΔH_f denoting the heat of fusion, ρ the density, D_m the diffusion coefficient of the melt, and V_n the normal growth velocity which is calculated by $V_n=V_p(\boldsymbol{n}_{ms}\cdot\boldsymbol{e}_z)$, with V_p the ampoule translate rate.

The boundary condition along the gas/ampoule surface involving heat transfer between the ampoule and furnace is given by

$$-(\nabla T)_a\cdot\boldsymbol{n}_{ag} = Rad[T^4 - T_f(z)^4] + Bi[T-T_f(z)],\ \text{on}\ \partial D_{ag}, \tag{6}$$

where T_f is the furnace temperature. The radiation number (Rad) and Biot number (Bi) are defined as $\varepsilon_{ag}\sigma T_{mp}R/k_a$ and hR/k_a, respectively, with ε_{ag} the emissivity, σ the Stefan-Boltzmann constant, h the convective heat transfer coefficient. The values of dimensionless groups used in this paper are gathered in Table 2.

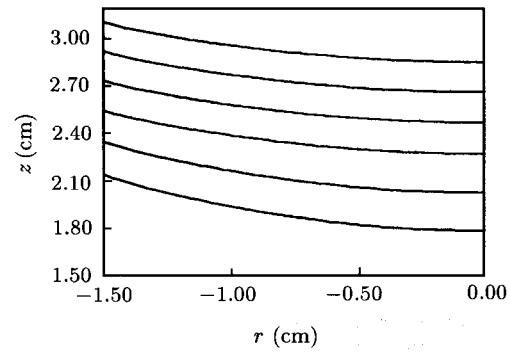


Fig. 3. Melt/crystal interface evolution at the initial moment of the growth. The time interval between two interface curves is 2500 s.

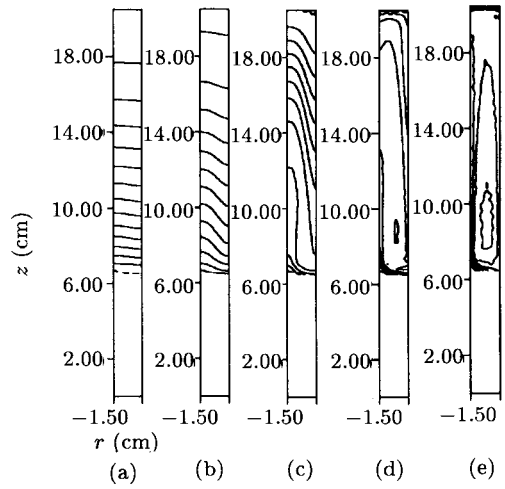


Fig. 4. Concentration field in whole domain under different gravity levels at $\tilde{t}=6.25\times10^4$ s. The dashed lines represent the melt/crystal interface: (a) $g=10^{-6}$, with $c_{max}=1.56$, $c_{min}=1.0$, $\Delta c=0.045$; (b) $g=10^{-5}$, with $c_{max}=1.62$, $c_{min}=1.01$ $\Delta c=0.05$; (c) $g=10^{-4}$, with $c_{max}=1.78$, $c_{min}=1.06$ $\Delta c=0.05$; (d) $g=10^{-3}$, with $c_{max}=1.89$, $c_{min}=1.14$ $\Delta c=0.05$; (e) $g=10^{-2}$, with $c_{max}=1.88$, $c_{min}=1.23$ $\Delta c=0.05$.

Finally, boundary conditions are supplied along the various inner surfaces of the ampoule for the temperature, velocity, and concentration fields. The detailed descriptions can be found in Refs. 3 and 4. And the initial conditions were given by the steady state solution under a stationary condition that the insulation zone of the furnace was kept from 1.5 to 6.5 cm along the z-direction.

Table 2. Dimensionless parameters and values for Te doped GaSb system.

Symbols	Definition	Values
Pr	v/α_m	0.016
Ra	$g_0 g\beta T_{mp}R^3/(\alpha_m\nu)$	$0-2.57\times10^{4*}$
Sc	ν/D_m	35.0
Pe_s	$RV_n\Delta H_f\rho_s/(k_sT_{mp})$	1.14×10^{-2}
Pe_c	RV_n/D_m	2.84
Rad	$\varepsilon_{ag}\sigma T_{mp}R/k_a$	1.18×10^{-7}
Bi	hR/k_a	1.37×10^{-2}

* Corresponding to the gravity factor g from 0 to 10^{-2}.

We employ Galerkin finite element method in the solution of the above model equations. Boundary conformal mapping technique[5] is applied to obtain the melt/crystal interface shape and position which is a

prior unknown, as well as the deformed finite element mesh in the whole domain. Mesh generation equations used here are the same as those used in Ref. 6. Details of our numerical techniques can be found in Refs. 4 and 6. All the calculations are carried out by 18×46 elements, with 32 elements along the z-direction in the melt region.

To demonstrate the robustness of our numerical algorithm, we try to reproduce two cases given in the literature: the result obtained by Talmon *et al.*[7] for a one-dimensional Stefan problem, and the result given by De Vahl Davis[8] for a standard natural convection problem in a square cavity. The physical models and parameters we use here are exactly the same as those of corresponding references. The calculation error for temperature field is estimated by

$$e_{\mathrm{rr}} = \left[\int_{\Omega}\left(T-\hat{T}\right)^2 \mathrm{d}\Omega\right]^{1/2} \Big/ \left(\int_{\Omega} T^2 \mathrm{d}\Omega\right)^{1/2}, \quad (7)$$

where Ω denotes the integral domain, $\hat{T}$ represents the 'standard' solution from Refs. 7 and 8, respectively. For the case of Ref. 8. we compare our result with the result obtained by using the finite element algorithm with a fixed mesh given in Ref. 8. Under the condition of $Ra = 1 \times 10^4$, $Pr = 0.71$, and 12×12 mesh, e_{rr} is 2.56×10^{-5}. Furthermore, we use 16×16 elements to calculate the temperature profiles in a slab of water at different times during freezing (Fig. 5 in Ref. 13). The calculation error e_{rr} is 6.77×10^{-3}.

A sequence of simulations is performed to demonstrate the combined effects of convection, segregation and melt/crystal interface shape for the Te doped GaSb growth system. The thermal field and solute concentration field with $g = 10^{-5}$ are given in Fig. 2. As solidification proceeds, Te is preferentially excluded from the crystal to melt because of $k < 1$, so that the solute concentration near the interface increases with time. While it seems that the shape of iso-thermal lines does not change too much during the growth except for the corresponding change with the moving of the interface (hence we only give one thermal field under a certain time). The melt/crystal interface is concave to the crystal because of the mismatch in the thermal conductivity between melt and crystal. We can notice the non-uniformity of the concentration distribution along the growth interface from Figs. 2(b)−2(d) under $g = 10^{-5}$ (the iso-concentration lines are curved). The compositional non-uniformity at the interface ξ is measured according to Ref. 9: $\xi = \left[(c_{\mathrm{I,max}} - c_{\mathrm{I,min}})/c_{\mathrm{I,ave}}\right]$ %, with $c_{\mathrm{I,ave}}$ the average concentration along the growth interface. We found that ξ only has a little change during the whole growth process. Figure 3 is the growth interface evolution at the beginning period of the growth. It is apparent that the growth interface becomes slightly flatter than the original one with increase of time, and gradually reaches a steady state. This transient change of the growth interface may be due to the coupling of the finite wall influence and little decrease of the flow intensity with time, because the flow pattern during the growth does not have too much change according to our calculations. The concentration distributions in the melt under different gravity levels are shown in Fig. 4. It can be seen that the concentration field is significantly deformed with the increase of the gravity, and a uniform cores even appear at $g = 10^{-3}$, with steep concentration gradients along the axial boundary which is consistent with the boundary-layer model for a well-mixed melt.[10] The compositional non-uniformity ξ at the growth interface is very small under $g = 10^{-6}$, and increases with the increase of gravity at low gravity levels. The ξ reaches a maximum at $g = 10^{-3}$ and decreases with the more intense flow motion (see Table 3). This result shows that when flow motion is strong enough, it turns out to be favorable to the uniform concentration distribution as long as it can keep steady. Similar result with Table 3 can be found in Ref. 11 for numerical study of Ga doped Ge growth.

Table 3. Change of compositional non-uniformity ξ with gravity factor g.

g	10^{-6}	10^{-5}	10^{-4}	10^{-3}	10^{-2}	5×10^{-2}
ξ(%)	0.18	2.35	6.53	8.69	7.33	7.12

In summary, we have performed a transient modeling of the Te doped GaSb melt growth process by using finite element method. The solute concentration at the growth interface increases with time because of $k < 1$. The temperature field and flow field are quite stable during the growth under our given conditions. We have found a transient region of the growth interface shape at the beginning of the growth. And after that the interface shape almost keeps unchanged which, together with the characteristic of flow and thermal fields, demonstrates the validity of quasi-steady state used on the investigations of crystal growth without dopants in the previous studies (see Ref. 12). Radial segregation occurs even under the condition of $g = 10^{-6}$. This segregation increases with the increase of gravity when gravity is small, and reaches a maximum at $g = 10^{-3}$ for our system. Next step of this research will carry out a systematic study on the influence of growth velocity, furnace temperature gradient, and direction of g-vector on the growth process in order to obtain an optimum growth condition for the future space flight.

REFERENCES

1 E. Lendvay *et al.*, J. Cryst. Growth, 71 (1985) 538.
2 CHEN Wan-chun, MAI Zhen-hong and K. Kato, Chin. Phys. Lett. 15 (1998) 613.
3 Liu Yong-cai *et al.*, Sci. Chin. 30 (2000) 79.
4 Yongcai Liu and Simon Brandon, J. Synthetic Crystals, 28 (1999) 8 (in Chinese).
5 K. Tsiveriotis and R. A. Brown, Inter. J. Numer. Fluids, 14 (1992) 981.
6 Y. C. Liu *et al.*, J. Cryst. Growth, 205 (1999) 333.
7 Y. Talmon *et al.*, AIChE J. 27 (1981) 928.
8 G. De Vahl Davis, *Natural convectin on a square cavity—a benchmark solution*, J. Numer. Meth. Fluids, 3 (1983) 249.
9 J. I. D. Alexander *et al.*, J. Cryst. Growth, 97 (1989) 285.
10 D. H. Kim *et al.*, J. Cryst. Growth, 114 (1991) 411.
11 C. J. Chang *et al.*, J. Cryst. Growth, 63 (1983) 343.
12 S. Brandon *et al.*, J. Derby, J. Cryst. Growth, 121 (1992) 473.
13 A. Van Mau *et al.*, Mat. Res. Bull. 7 (1972) 857.